University of Baghdad
College of Engineering
JE
JOURNAL OF ENGINEERING

Journal of Engineering
journal homepage: www.jcoeng.edu.iq
Volume 32 Number 11 November 2026



# A New Quaternary Blend for Eco-Friendly Foam Concrete

**Sara A. Hassan** , ***, Mohammed Zuhear Al-Mulali**

Department of Civil Engineering, College of Engineering, University of Baghdad, Baghdad, Iraq

## ABSTRACT

This study is about the Production of a sustainable and high - performance foamed concrete by using a quaternary binder system to substitute a part of ordinary Portland cement (OPC). The research investigates the replacement of cement by Class F fly ash (FA) as the main replacement material and ground granulated blast-furnace slag (GGBFS) and limestone powder ($CaCO_3$) as secondary replacement materials at replacement levels of 20%, 30% ,and 40% .All investigated mixes were designed mix proportion 1:1.2:0.45 with the fresh target density of 1350 ± 50 kg/m$^3$ for semi-structural applications. An extensive assessment was conducted in terms of fresh density, compressive strength, splitting tensile strength, carbonation depth, and microstructural characterization using scanning electron microscopy (SEM). SEM analysis observed that the 40% replacement level resulted in a dense microstructure with secondary C–S–H and C–A–S–H gels and refined pore structure. The results showed that the 40% quaternary substitution level provided a 28-day compressive strength of 9.00 MPa, exceeding that of the control mixture, with a good fresh density of 1345 kg/m$^3$ and improved foam stability. In contrast, it had higher splitting tensile strength but also had higher carbonation depth than control. Finally, these findings confirm 40% of quaternary binder as systematically sustainable and balanced alternative for the production of stable foamed concrete for semi-structural applications.

**Keywords:** Foamed Concrete, Quaternary Binder, Fly Ash, Sustainability, Compressive Strength.

## 1. INTRODUCTION

Concrete is the fundamental material used in construction worldwide and the second most consumed material on the earth after water. In 2021, the production of cement reached approximately 4.1 billion tons **(Abdullah et al., 2025)**. However, this massive consumption has significant environmental consequences due to the cement production industry being responsible for approximately 7% to 8% of the carbon dioxide emissions which is thereby contributing to the greenhouse phenomena **(Mehta and Monteiro, 2006; Vashistha et al., 2022)**. Therefore, the researcher goes to an innovative and sustainable solution: foamed concrete is defined as a light - weight concrete so this feature can reduce cement consumption, which is reflected on the production and transportation costs compared to conventional concrete **(Pandey et al., 2023; Alzlfawi, 2025)**. Foamed concrete is not only about reducing cement consumption, it also contributes to sustainability thanks to its properties that cut embodied and operational carbon emissions. The

*Corresponding author
Peer review under the responsibility of University of Baghdad.
https://doi.org/10.31026/j.eng.2026.11.11
This is an open access article under the CC BY 4 license (http://creativecommons.org/licenses/by/4.0/).
Article received: 11/05/2026
Article revised: 17/09/2026
Article accepted: 25/09/2026
Article published: 01/11/2026

cellular structure of the material is an effective thermal insulation which helps to reduce the long-term energy required for heating and cooling buildings **(Amran et al., 2015).** Furthermore, due to its low self-weight, the energy required for transportation can be reduced, and the size and material needs of structural foundations can be reduced, which indirectly reduces the carbon emissions associated with the support of structural members **(Gencel et al., 2022).**

Foamed concrete is produced by trapping air voids within a cement paste through the use of a compatible foaming agent **(Gencel et al., 2022; Zhang et al., 2023)**. Foamed concrete is different from lightweight concretes by its production process which incorporates foam with a mortar to create a self-compacting concrete with high followability and air bubbles which create air voids **(Ramamurthy et al., 2009)**. The air-voids structure strongly influences foamed concrete performance, with densities of (600–1900) kg/m$^3$, air-voids contents of 10–70%, and compressive strengths of 2–58MPa **(Wee et al., 2006)**. Its lower density than conventional concrete typically 1000–1600 kg/m$^3$ also provides improved fire resistance and thermal and acoustic insulation **(Awang and Aljoumaily, 2017)**. For semi-structural applications, densities of 800–1200 kg/m$^3$ are commonly used in partition walls, bricks, and parapets **(Amran et al., 2015; Gencel et al., 2022)**, while higher-density foamed concrete has been applied in shear walls and railway trackbeds due to its reduced self-weight and controlled deformation **(She et al., 2018; Fu et al., 2020)**. It is also used in geotechnical applications, including deformable tunnel-lining backfill to accommodate swelling pressures **(Fu et al., 2020)**.

The experimental results have found that a matrix that is characterized by tiny, individual air voids, compare with matrix with a large and interconnected void, significantly enhances the structural integrity and strength-to-weight ratio of the compound material **(Wee et al., 2006; Huy and Hong, 2022)**. Also, improvements in foaming agents, e.g. animal proteins, a more stable and closed-air void structure compared to synthetic foaming agents, integrity retained during hydration **(Remadnia et al., 2009)**.

To achieve sustainability, researchers have found out the incorporation of Supplementary Cementitious materials (SCMs) such as fly ash, ground granulated blast furnace slag (GGBFS), oil palm ash **(Mydin et al., 2023)**. Replacement of high volumes of cement—up to 67% or even 75%—solely with fly ash often leads to an unfavorable reduction in early-age and ultimate compressive strengths of well-cured specimens due to slow initial hydration kinetics **(Kearsley and Wainwright, 2001).** Furthermore, the selection of fillers is vital; utilizing fine materials or substituting fly ash for sand as a micro-filler markedly enhances the strength-to-density ratio due to pozzolanic activity, which refines the cell walls between air voids **(Nambiar and Ramamurthy, 2006).** SCMs can be used as individual materials or as an integrated blend such as binary **(Güneyisi and Gesoğlu, 2008),** ternary **(Gopalakrishnan et al., 2019)** and quaternary systems **(Chan and Zhang, 2023)** The quaternary replacement system, which is the combination of three different supplementary cementitious materials (SCMs) with ordinary Portland cement (OPC), is an extremely effective method to enhance both environmental performance and concrete properties **(Huy and Hong, 2022; Chan and Zhang, 2023)** .Each component has its own role: Fly ash increases workability and pozzolanic reaction **(Qu et al., 2022)**; GGBFS improves strength and durability **(Sebastian and VR, 2021)** and limestone powder is a filler that densifies the microstructure and accelerates early hydration **(Aslan and Erkan, 2024).** As a result, foamed concrete has changed from being a simple insulator to a functional structural element, such as one-way ribbed slabs, which greatly reduce dead loads, and, by decreasing the size of columns and footings, offer economic benefits **(Abdellatief et al., 2025)**. However, these developments still have limitations for the optimization of binder

systems for foamed concrete. This is because foamed concrete does not include coarse aggregate, and that often needs careful cement binder proportioning. However, the environmental footprint of foamed concrete can be effectively mitigated and minimized by using sustainable quaternary blended systems with significant reduction in the net Ordinary Portland Cement (OPC) consumption **(Abdulazeez and Sani, 2026)**. Foamed concrete (FC) commonly includes supplementary cementitious materials (SCMs). However, existing research work mainly focuses on binary or ternary replacement systems **(Gopalakrishnan, et al., 2019; Lin et al., 2023)**. Also mentioned is that incorporating nano-materials such as nano-$TiO_2$ improves the interfacial transition zone, leading to the increment of tensile strength of foamed concrete **(Salman and Al-Mulali, 2025).**

Therefore, this study aims to fill this research gap by experimentally investigating the performance of foamed concrete in a quaternary replacement system composed of Cement, Fly Ash, GGBFS, and Limestone powder. The novelty of this research is evaluating the synergistic interaction among these binder components and its impact on compressive strength, splitting tensile strength, carbonation depth, fresh density and SEM analysis while reducing cement consumption and improving sustainability.

The methodology to assess the proposed quaternary replacement system in foamed concrete is systematically conducted via three successive phases such as material preparation, molding and testing. The plan of this research was based on the measurement of fresh density after mixing, and then the testing of hardened properties at 7 and 28 days of curing. The mechanical development and durability are completely assessed by testing for the compressive strength, splitting tensile strength and carbonation depth for the evaluation of hardened state. The structured methodology by SEM is proposed to provide conclusive results on the effect of cementitious substitution on the high foamed concrete performance and Achieving Sustainability with semi-structure characteristics.

## 2. MATERIAL AND METHODS

### 2.1 Materials

#### 2.1.1 Cement(c)

OPC CEM I-42.5R, in accordance to **(IQS No. 5, 2019)** was used throughout this study**. Tables 1 and 2** list the chemical composition and physical properties, respectively.

**Table 1.** Cement's chemical composition

| Oxide composition | Test Result (%) | (IQS No. 5, 2019) Limits |
|---|---|---|
| Lime (CaO) | 62.5 | ------ |
| Silica ($SioO_2$) | 21.27 | ------ |
| Iron oxide($Fe_2O_3$) | 3.68 | ------ |
| Aluminum Oxide ($Al_2O_3$) | 4.04 | ------- |
| Magnesium Oxide (MgO) | 2.20 | ≤5% |
| Sulfur Trioxide ($SO_3$) | 2.47 | 2.8max if $C_3A$> 3.5 % |
| Loss on Ignition L.O.I | 1.43 | Max4% |
| Insoluble-residue (I.R.) | 0.69 | Max1.5 |
| Initial Setting Time | 131 | ≥45 MIN |
| Major compounds of cement | | |
| Dicalcium Silicate($C_2S$) | 8.31 | Bogue equation according to **(ASTM C150/150M -24, 2024)** |
| Tricalcium Silicate($C_3S$) | 66.32 | |
| Tricalcium Aluminate ($C_3A$) | 4.49 | |

**Table 2.** Cement's Physical properties

| Properties | Test result | (IQS No. 5, 2019 ) Limits |
|---|---|---|
| Final Setting Time | 5:10 | ≤10:00 HR |
| Compressive Strength (2-Day) | 24.12 | ≥20.MPA |
| Compressive Strength (28-Day) | 44.37 | 42.5≤MPA |

### 2.1.2 Fly Ash (FA)

In this study, class F fly ash conforming to **(ASTM C618-25, 2025)** was used in all the mixes containing the quaternary binder. The particle size distribution was analyzed via the Laser Diffraction Method (Shimadzu SALD-2300) and its chemical composition quantified using Energy Dispersive X-ray Spectroscopy (EDX), as detailed in **Tables 3 and 4.** The physical properties of the fly ash are provided in **Appendix A**

**Table 3.** Fly Ash chemical composition

| Oxide composition | Test Result (%) | (ASTM C618-25, 2025) Limits |
|---|---|---|
| Aluminum Oxide ($Al_2O_3$) | 17.406 | Sum not less than 50% |
| Iron Oxide ($Fe_2O_3$) | 12.613 | |
| Silica ($SiO_2$) | 65.32 | |
| Calcium Oxide (CaO) | 6.961 | Max18 |
| Sulfur Trioxide ($SO_3$) | 2.162 | Max 5% |
| Manganese Oxide (MgO) | 0.139 | |

**Table 4.** Particle size distribution of the fly ash used in this study

| Physical Parameter | | Result |
|---|---|---|
| Median Diameter D50 | | 33.627µm |
| Particle Size D25 | | 12.893µm |
| Particle Size D75 | | 156.501µm |
| Absorbance | | 0.177 |
| Activity index @7 day | 89 | Min75% |
| Activity index @28 day | 106.2 | Min75% |

### 2.1.3 Lime Stone ($CaCO_3$)

Lime stone powder ($CaCO_3$) conforming to **(ASTM C1797-17, 2017)** was utilized in this study. The particle size distribution was analyzed via the Shimadzu SALD-2300 laser diffraction system and its physicochemical properties detailed in **Tables 5 and 6.**

**Table 5**. Lime stone chemical composition

| Oxide composition | Test result (%) | (ASTM C1797-17, 2017) Limits |
|---|---|---|
| Calcium Oxide (CaO) | 87.737 | |
| Silicon Dioxide ($SiO_2$) | 6.053 | |
| Magnesium Oxide (MgO) | 2.109 | Max 5 |
| Aluminum Oxide ($Al_2O_3$) | 1.451 | |
| Sulfur Trioxide ($SO_3$) | 1.34 | |
| Iron Oxide ($Fe_2O_3$) | 0.497 | |

**Table 6**. Particle size distribution

| Physical Parameter | Results |
|---|---|
| Median Diameter D50 | 289.653µm |
| Particle Size D25 | 245.062µm |
| Particle Size D75 | 345.403µm |
| Absorbance | 0.281 |

### 2.1.4 Ground Granulated Blast-Furnace Slag (GGBFS)

GGBFS conforming to **(ASTM C989-22, 2022)** was used in this study. particle size distribution was analyzed using the Shimadzu SALD-2300 laser diffraction system and its physicochemical properties detailed in **Tables 7 and 8.**

**Table 7.** Chemical Composition of GGBFS

| Oxide composition | Test result (%) | (ASTM C989-22, 2022) Limits |
|---|---|---|
| Calcium Oxide (CaO) | 50.568 | |
| Silicon Dioxide ($SiO_2$) | 28.623 | |
| Magnesium Oxide (MgO) | 1.246 | Max 15 |
| Aluminum Oxide ($Al_2O_3$) | 7.599 | |
| Sulfur Trioxide ($SO_3$) | 2.167 | Max 2.5 |
| Iron Oxide ($Fe_2O_3$) | 2.136 | |
| Titanium dioxide ($TiO_2$) | 3.009 | |
| Manganese dioxide (MnO) | 2.568 | |
| Potassium oxide($K_2O$) | 1.415 | |

**Table 8.** Physical properties of GGBFS

| Physical Parameter | | Result |
|---|---|---|
| Median Diameter D50 | | 21.981µm |
| Particle Size D25 | | 10.874µm |
| Particle Size D75 | | 45.145. µm |
| Absorbance | | 0.133 |
| Activity index @7 day | 70 | ------- |
| Activity index @28 day | 78 | Min75% grade 80 |

### 2.1.5 Foaming Agent

The protein-based surfactant foaming agent used in this study is known as Genfil and is manufactured by ARTRA. DRN provided the foaming agent. The foaming agent was diluted with water at a ratio of 1:30. The diluted solution was aerated with a foam generator to produce stable foam. The density of the liquid foaming agent is 80-90kg/m$^3$. The main Characteristics of the foaming agent were summarized in **Table 9** as presented by manufacture. A foam generator was employed to produce stable foam as shown in **Fig. 1**

**Table 9.** Foam properties

| Parameter | Result |
|---|---|
| Physical state and appearance | Dark brown liquid |
| Density | 1.05 kg/L |
| PH –value | 6 – 7 |
| Solubility in water | Soluble |
| Dry matter content | 6.5% |
| Ash content | 0.6% |
| Flammability | Non-flammable |



(a)



(b)

**Figure 1.** (a) Foaming Machine (b) Stable foam

2.1.6 Sand

The fine aggregate used in this study is natural sand conforming to Iraqi Standard Specification **(IQS No. 45,1984**). The sieve analysis and chemical properties of the sand are presented in **Tables 10 and 11**, respectively.

**Table 10.** Sieve analysis of the fine aggregate used in this study

| Sieve size mm | %passing | Limits of (IQS No. 45,1984) (Zone 4) |
|---|---|---|
| 10 | 100 | 100 |
| 4.75 | 100 | 95-100 |
| 2.36 | 100 | 95-100 |
| 1.18 | 100 | 90-100 |
| 0.60 | 82.4 | 80-100 |
| 0.30 | 17 | 15-50 |
| 0.15 | 7 | 0-15 |

**Table 11.** Fine aggregate's chemical properties

| Property | Result |
|---|---|
| finesse modulus | 1.93 |
| Specific gravity | 2.4 |
| Absorption | 1.16 |
| Dry density | 1600 Kg/m$^3$ |
| Sulfate content $SO_3$ | 0.38 % max 5 |

## 2.2 Experimental Work

2.2.1 Mix Constituents

All of the foamed concrete mixes used in this study were prepared with a constant mix proportion. The binder system was quaternary, using fly ash (FA) as the primary cement replacement and ground granulated blast-furnace slag (GGBFS) and limestone powder ($CaCO_3$) as secondary constituents. The density of the base mortar before the addition of the preformed foam was approximately 2100 kg/m$^3$. Foam was added in different quantities to reach a new target density of 1350 ± 50 kg/m$^3$, the target density range for semi-structural corresponding to an approximate target oven–dry 1200± 50 kg/m$^3$. To achieve this target density, a design foamed (316) Liter was determined. The ratio of binder: sand: water was maintained the same for all the mixes of 1:1.2:0.45, and the percentage of total cement replacement varied from 0% to 40% as given in **Table 12**

**Table 12.** Mix constituents per cubic meter of foam concrete

| Mixes | *R.L (%) | Cement (kg) | Sand (kg) | Fly Ash (kg) | GGBFS (kg) | $CaCO_3$ (kg) | Design Water(kg) | Actua-l water(kg) | Actual Foamed(L) |
|---|---|---|---|---|---|---|---|---|---|
| FA-0 | 0 | 500 | 600 | 0 | 0 | 0 | 225. | 202.2 | 405 |
| FA-20 | 20 | 400 | 600 | 62.50 | 12.50 | 25.00 | 225 | 209.5 | 410 |
| FA-30 | 30 | 350 | 600 | 75.00 | 25.00 | 50.00 | 225 | 211.6 | 410 |
| FA-40 | 40 | 300 | 600 | 87.50 | 37.50 | 75.00 | 225 | 215.4 | 410 |

*R.L Represented replacement level

2.2.2 Mixing Procedure

After preparing all the materials, sand was fed into the mixer, and 10% of the calculated water was added along with the sand. Afterwards, the cementitious material was added to the sand and water; the mixer was then operated for 3 to 4 minutes to achieve a homogenous mixture. The remaining water was added gradually to the mortar mix until a density of approximately 2100 kg/m$^3$ was achieved. This density was checked by weighing a standard one-liter cup of the mortar. Pre-formed foam was injected into the mortar to achieve the target fresh density. after the foam was fully blended, the final fresh density was checked to ensure that it is within the range of 1350 ± 50 kg/m$^3$. Finally, the concrete was cast into clean, oiled molds. After 24 hours, the specimens were demolded and immediately wrapped in plastic sheets in accordance to (**Kearsley, 2006).**

## 3. PROGRAM TEST

### 3.1 Compressive Strength

The compressive strength was determined according to **(BS EN 12390-3, 2019)** using cubic specimens with dimensions of 100 ×100 mm. Testing was conducted at 7 and 28 where the average of three specimens was taken to ensure reliability. The strength (*Fc*) was calculated as mentioned in Eq. (1).

$$Fc = \frac{F}{A} \quad (1)$$

Where:

Fc = the compressive strength (MPa),
F=is the maximum load at failure (N),
Ac= is the cross-sectional area of the specimen (mm$^2$)

### 3.2 Splitting Tensile Strength Test

The splitting tensile strength was determined according to **(BS EN 12390-6, 2023).** Cylindrical specimens having a diameter of 100 mm and height of 200 mm were used. Testing was conducted at 7 and 28, with the average of three samples recorded for each age. The splitting tensile strength was calculated using Eq. (2)

$$Fct = \frac{2p}{\pi LD} \quad (2)$$

Where:

$Fct$ = splitting tensile strength (MPa).
$p$ = maximum load applied by the testing machine at the moment of failure, measured (N).
L=the length of the cylindrical specimen (mm).
D= the diameter of the cylindrical specimen (mm)

### 3.3. Fresh Density

The fresh or "as-cast" density was determined immediately after the mixing process in accordance with **(BS EN 12350-6, 2019)** This measurement is essential to verify the stability of the foam and to ensure the target wet density is achieved. The wet density (wet) was calculated by filling a container of a known volume with the fresh foamed concrete and its density was recorded using Eq. (3):

$$\text{Wet density} = \frac{Wf - Wc}{V} \quad (3)$$

Where:
Wet density represented is the fresh (wet) density of the foamed concrete (kg/m$^3$).
$Wf$ is the weight of the container filled with fresh foamed concrete (kg).
$Wc$ is the weight of the empty container (kg).
V: is the internal volume of the container (m$^3$).

### 3.4 Carbonation Depth

According to **(BS EN 14630, 2021**), carbonation depth was measured at 7 and 28 days by spraying a 1% phenolphthalein indicator onto freshly broken prism faces. After 30seconds the depth of $CO_2$ penetration based on the discoloring that occurs where areas with a pH above 9 turned a distinct red-purple, while the carbonated parts remained colorless. The average depth was measured using a Vernier caliper.

### 3.5 Microstructural Analysis

The microstructural characteristics of the selected foamed concrete mixtures were investigated using scanning electron microscopy (SEM) to examine the morphology, pore structure, and hydration products of the quaternary binder matrix. Small fragments were collected from the fractured specimens and prepared for SEM analysis to characterize the microstructural features associated with the different replacement levels.

## 4. RESULTS AND DISCUSSION

### 4.1 Mechanical Strength

**Table 13** shows the results for the strength (compressive and splitting tensile strength) at the ages of 7 and 28 days for for the prepared foamed concrete mixes. From the first observation, the strength increased with age for all replacement levels. At 7 days, the highest strength was obtained by the control mix followed by 40%, 20%, and 30%, respectively. The strength decreased with the increase in replacement levels except for the specimens containing a 40% replacement level. The control mix obtained the highest compressive strength of 6.9 MPa and 1.02 MPa splitting tensile strength. This is attributed to the high quantity of activate binder (cement), lower water content (202.2 Kg) that led to produce specimens with dense less porous matrix. This is clearly evident by the high oven-dry density readings shown in **Table 13 (Ahmed, 2024)**.

At 20% and 30% replacement levels, the lowest compressive and splitting tensile strengths were observed compared to the control. The decrease in the cement quantity, the early dilution effect, not enough $CaCO_3$ for it to work as a packing filler, synergistic effect, and the increase in water and foam content caused a reduction in oven-dry density leading to a reduction in strength at these replacement levels **(Gencel et al., 2022; Abdulazeez and Sani, 2026)**.

In contrast to the 20 and 30%, foam concrete mixes containing 40% cement substitution of quateranry blend showed a clear adverse trend, obtaining better compressive and tensile strengths. Despite of having a higher water content. This improvement is related to the sufficient amount of $CaCO_3$ that improved the particle packing and facilitated synergistic interactions among the components of the quaternary binder system. These effects have contributed to the development of more calcium silicate hydrate (C-S-H) and calcium aluminate hydrate (C-A-H) gels, resulting in a denser microstructure and higher oven-dry density of 1240 kg/m$^3$ **(De Weerdt et al., 2011; Schöler et al., 2015)**. At 28 days, the mix containing a 40% replacement level achieved the highest compressive and splitting tensile strengths (9) and (1.35) MPa **respectively**. By that exceeding the control mix's readings by 5.88% and 11.6% in compressive and splitting tensile strength, respectively.

**Table 13.** compressive and splitting tensile strength development at different replacement levels and curing age

| Mixes | R.L(%) | Oven-dry density (Kg/m$^3$) | | Compressive strength (MPa) | | Splitting tensile strength (MPa) | |
|---|---|---|---|---|---|---|---|
| Age (days) | | 7 | 28 | 7 | 28 | 7 | 28 |
| FA-0 | 0 | 1233 | 1235 | 6.9 | 8.5 | 1.02 | 1.21 |
| FA-20 | 20 | 1190 | 1195 | 5.06 | 5.30 | 0.54 | 0.80 |
| FA-30 | 30 | 1185 | 1190 | 4.20 | 4.60 | 0.63 | 0.67 |
| FA-40 | 40 | 1240 | 1243 | 6.50 | 9.00 | 0.77 | 1.35 |

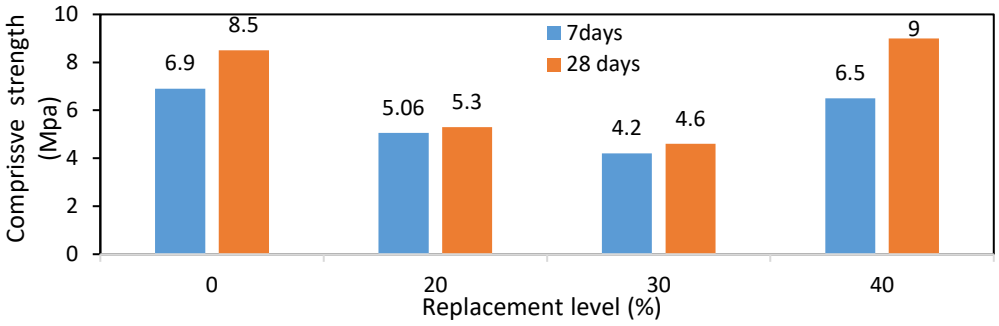



**Figure 2.** Compressive strength result

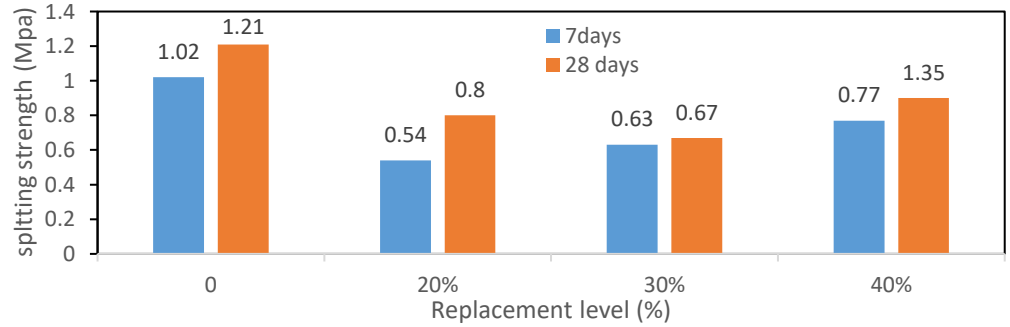



**Figure 3.** Splitting Tensile Strength result

### 4.2 Carbonation Depth

As shown in **Fig. 4**, the experimental results show that the carbonation depth of the quaternary foamed concrete mixtures increases progressively with the increase in the substitution ratio from 20% to 40%. At 7 days of age, carbonation depth increased from 0.1 mm in the control mix to 0.125 mm, 0.127 mm, and 0.135 mm for 20%, 30% and 40% replacement levels, respectively. A similar increasing trend was observed after 28 days; the maximum carbonation depth (0.142 mm) was at 40% substitution ratio as compared to the control (0.124 mm).

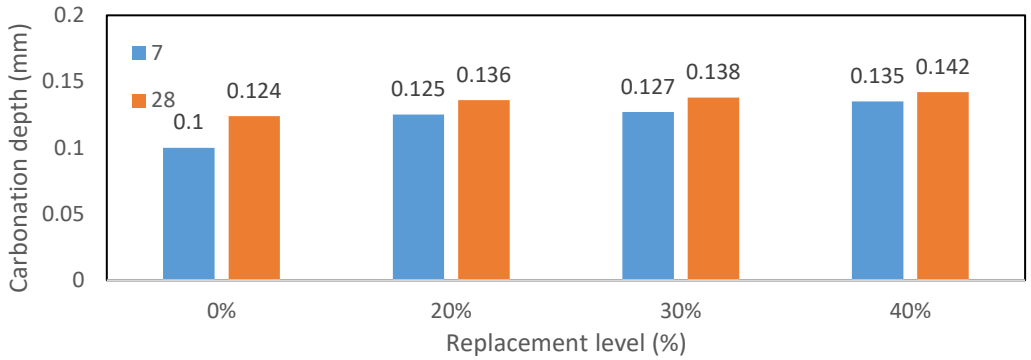



**Figure 4.** Carbonation depth result

This increase is directly related to the increase in $CaCo_3$ and water content **(Justens, 2016),** which is a major contributor to the reduction of carbonation resistance. This is because the substitution of Portland cement reduces the amount of calcium hydroxide, $Ca(OH)_2$, available and therefore the chemical buffering capacity against the ingress of atmospheric $CO_2$ is reduced. Hence, with the increase in the ratio of quaternary substitution and curing age, the decrease in alkalinity of the system makes it easier for the carbonation front to penetrate deeper into the concrete matrix **(Herath et al., 2020).**

### 4.3 Fresh Density

In this study, a precise amount of pre-formed foam was used and adapted for each mix to achieve the specified target fresh density 1350 ± 50 Kg/m$^3$. of density. **Fig. 5** shows the fresh density readings of the prepared foam concrete mixes. Depending on actual water and foam content, a fluctuant trend was observed to obtain the designated target fresh density. Foam concrete mixes containing replacement levels of 20% and 30% obtained 1290 kg/m$^3$ and 1320 kg/m$^3$ respectively compared to the control mix's 1340 kg/m$^3$.

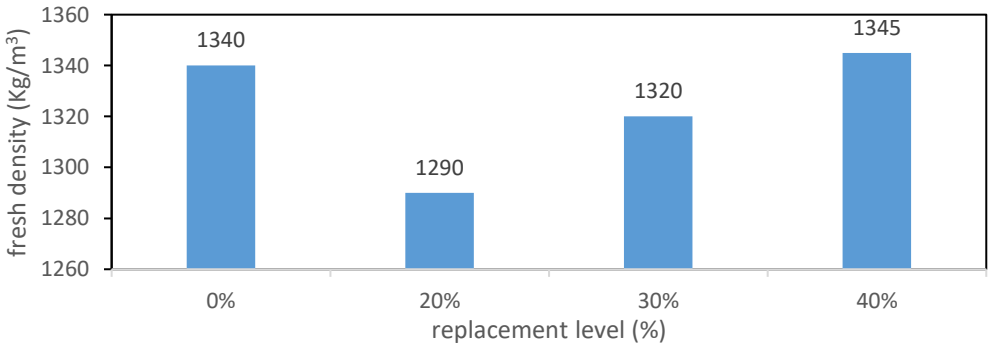
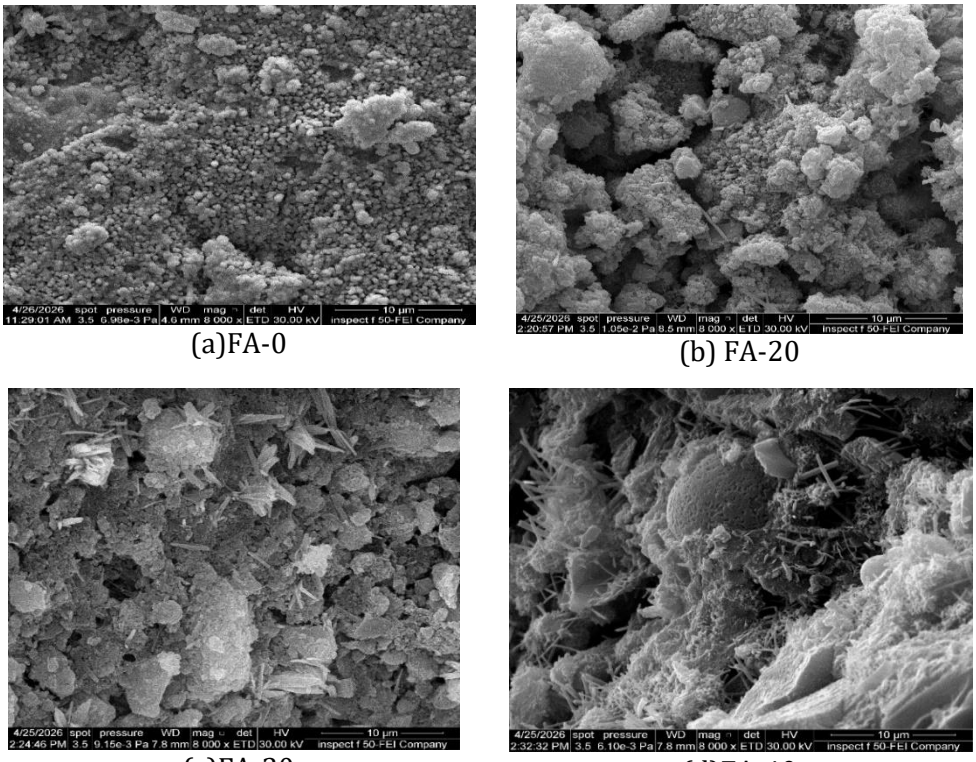



**Figure 5.** Fresh density for each foam concrete mix

The 40% replacement level reached a maximum density of 1345 kg/m$^3$. The higher fresh density at the 40% level, even with the increased foam quantity, indicated better foam stability and an optimized air-void system. The main reason for this behavior is the synergistic effect of limestone powder and fly ash, which improves the plastic viscosity of the cement paste **(Nordin et al., 2014).** The increased viscosity effectively coats the air bubbles and prevents their coalescence such that the integrity of the matrix and the target casting density are maintained during the process **(Jin et al., 2011).** Hence, the best blend threshold for a consistent foam concrete mix.

### 4.4 Microstructure

**Fig. 6** shows SEM micrograph images of the foamed concrete mixes at 28 days with a magnification of 8000x. A noticeable microstructural development throughout the quaternary blends, from the control mix to the 40% replacement level. The control mix showed the densest matrix with features consistent with the early Portlandite $Ca(OH)_2$ plates and initial C-S-H gel observed in the control mixture, which results in the highest splitting tensile strength of 1.21MPa and the lowest carbonation depth of 0.124 mm, but no spatial pore refinement in the long term (**Compaoré et al., 2023; Gong and Zhang, 2019)**.



(a)FA-0 (b) FA-20

(c)FA-30 (d)FA-40

**Figure 6.** SEM micrographs of foamed concrete mixes at 28 days (magnification: 8,000x)

Moving to the 20% replacement level, the matrix shows irregular agglomerates and more clearly interconnected capillary pores resulting from early clinker dilution, which explains the sharp drop in mechanical strengths and an increased carbonation depth of 0.136mm. The reduction in early performance is in agreement with the clinker dilution effect **(Mydin et al., 2023; Zhang et al., 2026).** The 30% replacement level produces a porous microstructure and increased bleeding channels with increasing actual water demand, which results in a reduction in mechanical performance and increases the carbonation depth

to 0.138 mm, indicative of the fresh-state and rheological challenges normally encountered when the water-to-binder ratio is not optimized in SCM-blended systems **(Mohd Fauzi et al., 2020; Zhang et al., 2022)**. Finally, significant change of the microstructure occurs to a dense matrix with features consistent with secondary C-S-H with tightly embedded fly ash, GGBS and limestone fillers achieving this packed matrix in which it interrupts the continuous capillary paths. This may explain the achieved superior mechanical properties at the age of 28 days, and successfully stabilizes the carbonation front despite the consumption of $Ca(OH)_2$, which is consistent with the pore refinement, micro-filling, and nucleation mechanisms reported for optimized mineral admixture combinations **(Vishavkarma et al., 2024; Jones et al., 2016)**.

## 5. CONCLUSIONS

The findings of this study on quaternary foamed concrete lead to the following conclusions:

- A sustainable and eco-friendly foamed concrete is produced by utilizing a quaternary binder system where Fly ash is the main substitution material, thus reducing the total cement content
- The most effective replacement level was found to be 40% which gave a compressive strength of 9 MPa at 28 days which was higher than the 8.5 MPa compressive strength exhibited by the control mix.
- At the age of 28 days, the splitting tensile strength of 1.35 MPa at the 40% substitution level provided further confirmation of the mechanical integrity, indicating a strong internal framework and improved cohesion within the solid matrix.
- At the 40% level of the quaternary blend, the maximum fresh density was 1345 kg/m$^3$ with the best foam stability and the excellent air-void system due to the increased plastic viscosity of the quaternary binder paste.
- Despite the improvement in mechanical performance, the high substitution rate caused a progressive increase in carbonation depth, reaching a maximum of 0.142 mm at 28 days for the 40% mix.
- SEM microstructural analysis confirmed that the 40% quaternary blend—incorporating fly ash, GGBFS, and limestone powder—successfully transformed the internal matrix into a dense, interlocked structure enriched with secondary C–S–H and C–A–S–H gels, effectively refining pore pathways and enhancing matrix densification.
- The study validates that a 40% quaternary substitution is a viable eco-friendly solution, preserving and even improving high-performance characteristics suitable for semi-structural applications while significantly reducing the environmental impact of concrete production

### Credit Authorship Contribution Statement

Sara. A. Hassan: Visualization, Writing draft, discussion Validation, Methodology. Mohammed Zuhear Al-Mulali: Supervision, editing, and reviewing

### Declaration of Competing Interest

The authors declare that they have no known competing financial interests or personal relationships that could have appeared to influence the work reported in this paper.

## REFERENCES

Abdellatief, M., Hassanien, A.E., Mortagi, M. and Hamouda, H., 2025. Geopolymer foam concrete: a review of pore characteristics, compressive strength and artificial intelligence in GFC strength simulations. *Discover Concrete and Cement*, 1(1). https://doi.org/10.1007/s44416-025-00003-x

Abdulazeez, A.S. and Sani, A.A., 2026. Properties of foam concrete: a review. *Discover Concrete and Cement*, 2(4), pp. 1–30. https://doi.org/10.1007/s44416-026-00042-y

Abdullah, A.F., Ezuldin, N.Y., Ahmed, I.M. and Al-Khafaji, Z., 2025. Enhancing the sustainability of concrete mixes utilizing supplementary cementitious materials in renewable energy buildings. *Engineering, Technology and Applied Science Research*, 15(5), pp. 28041–28049. https://doi.org/10.48084/etasr.12936

Ahmed, A., 2024. Assessing the effects of supplementary cementitious materials on concrete properties: A review. *Discover Civil Engineering*, 1(145). https://doi.org/10.1007/s44290-024-00154-z

Alzlfawi, A., 2025. Microstructural and mechanical characterization of foamed concrete reinforced with scrap aluminum engine residue. *Scientific Reports*, 15(1). https://doi.org/10.1038/s41598-025-16494-4

Amran, Y.H.M., Farzadnia, N. and Abang Ali, A.A., 2015. Properties and applications of foamed concrete; a review. *Construction and Building Materials*, 101, pp. 990–1005. https://doi.org/10.1016/j.conbuildmat.2015.10.112

Aslan, S. and Erkan, İ.H., 2024. The effects of fly ash, blast furnace slag, and limestone powder on the physical and mechanical properties of geopolymer mortar. *Applied Sciences*, 14(2), P. 553. https://doi.org/10.3390/app14020553

ASTM C150/C150M-22, 2024. Standard Specification for Portland Cement. West Conshohocken, PA: ASTM International. https://doi.org/10.1520/C0150_C0150M-22

ASTM C618-25a, 2025. Standard Specification for Coal Fly Ash and Raw or Calcined Natural Pozzolan for Use in Concrete. West Conshohocken, PA: ASTM International. https://doi.org/10.1520/C0618-25A

ASTM C989/C989M-22, 2022. Standard Specification for Slag Cement for Use in Concrete and Mortars. West Conshohocken, PA: ASTM International. https://doi.org/10.1520/C0989_C0989M-22

ASTM C1797-17, 2017. Standard Specification for Ground Calcium Carbonate and Aggregate Mineral Fillers for Use in Hydraulic Cement Concrete. West Conshohocken, PA: ASTM International. https://doi.org/10.1520/C1797-17

Awang, H. and Aljoumaily, Z.S., 2017. Influence of granulated blast furnace slag on mechanical properties of foam concrete. *Cogent Engineering*, 4, 1409853. https://doi.org/10.1080/23311916.2017.1409853

BS EN 12390-3:2019, 2019. Testing Hardened Concrete. Compressive Strength of Test Specimens. British Standards Institution. https://doi.org/10.3403/30360097

BS EN 12390-6:2023, 2023. Testing Hardened Concrete. Tensile Splitting Strength of Test Specimens. British Standards Institution. https://doi.org/10.3403/30454320

BS EN 12350-6:2019, 2019. Testing fresh concrete – Part 6: Density. British Standards Institution. https://doi.org/10.3403/30360091

BS EN 14630:2021, 2021. Products and Systems for the Protection and Repair of Concrete Structures. Test Methods. Determination of Carbonation Depth in Hardened Concrete by the Phenolphthalein Method. British Standards Institution. https://doi.org/10.3403/30091526U

Chan, C.L. and Zhang, M., 2023. Effect of limestone on engineering properties of alkali-activated concrete: A review, Construction and Building Materials, 362, P. 129709. https://doi.org/10.1016/j.conbuildmat.2022.129709

Compaoré, A., Sawadogo, M., Sawadogo, Y., Ouedraogo, M., Sorgho, B., Seynou, M., Blanchart, P. and Zerbo, L., 2023. Preparation and characterization of foamed concrete using a foaming agent and local mineral resources from Burkina Faso. *Results in Materials*, 17, 100365. https://doi.org/10.1016/j.rinma.2023.100365

De Weerdt, K., Kjellsen, K.O., Sellevold, E. and Justnes, H., 2011. Synergy between fly ash and limestone powder in ternary cements. *Cement and Concrete Composites*, 33(1), pp. 30–38. https://doi.org/10.1016/j.cemconcomp.2010.09.006

Fu, Y., Wang, X., Wang, L. and Li, Y., 2020. Foam concrete: A state-of-the-art and state-of-the-practice review, Advances in Materials Science and Engineering, 2020, Art. ID 6153602, pp. 1-25. https://doi.org/10.1155/2020/6153602

Gencel, O., Bilir, T., Bademler, Z. and Ozbakkaloglu, T., 2022. A detailed review on foam concrete composites: ingredients, properties, and microstructure. *Applied Sciences*, 12(11), P. 5752. https://doi.org/10.3390/app12115752

Gong, J. and Zhang, W., 2019. The effects of pozzolanic powder on foam concrete pore structure and frost resistance. *Construction and Building Materials*, 208, pp. 135–143. https://doi.org/10.1016/j.conbuildmat.2019.02.021

Gopalakrishnan, R., Sounthararajan, V., Mohan, A. and Tholkapiyan, M., 2019. The strength and durability of fly ash and quarry dust light weight foam concrete. *Materials Today: Proceedings*, 22, pp. 1117–1124. https://doi.org/10.1016/j.matpr.2019.11.317

Güneyisi, E. and Gesoğlu, M., 2008. Properties of self-compacting mortars with binary and ternary cementitious blends of fly ash and metakaolin. *Materials and Structures*, 41(9), pp. 1519–1531. https://doi.org/10.1617/s11527-007-9345-7

Herath, C., Gunasekara, C., Law, D.W. and Setunge, S., 2020. Performance of high volume fly ash concrete incorporating additives: A systematic literature review. Construction and Building Materials, 258, P. 120606. https://doi.org/10.1016/j.conbuildmat.2020.120606

Huy, N.S. and Hong, M.T., 2022. The influence of fly ash and foam contents on the properties of lightweight foamed concrete. *Vietnam Journal of Science, Technology and Engineering*, 64(2), pp. 42–49. https://doi.org/10.31276/VJSTE.64(2).42-49

Iraqi Standard Specification No. 45, 1984. Aggregate specifications. Baghdad: Central Agency for Standardization and Quality Control.

Iraqi Standard Specifications No. 5, 2019. Portland Cement Specialties. Baghdad: Central Organization for Standardization and Quality Control.

Jia, Y., Aruhan, B. and Yan, P., 2004. Natural and accelerated carbonation of concrete containing fly ash and GGBS after different initial curing period. *Magazine of Concrete Research*, 64(2), pp. 143–150. https://doi.org/10.1680/macr.10.00134.

Jones, M.R. and McCarthy, A., 2005. Utilising unprocessed low-lime coal fly ash in foamed concrete. *Fuel*, 84(11), pp. 1398–1409. https://doi.org/10.1016/j.fuel.2004.09.030

Jones, M.R., Zheng, L. and Mohammed, M., 2016. Bubble Structure, Stability and Rheology of Foamed Concrete. In: The 9th International Concrete Conference 2016. University of Dundee, pp. 682–694.

Jin, M.T., Huang, C.J. and Jin, Z.F., 2011. The physical and chemical properties of fly ash from municipal solid wastes incineration. Advanced Materials Research, 194–196, pp. 2065–2071. https://doi.org/10.4028/www.scientific.net/amr.194-196.2065

Justnes, H., 2016. How SCMs improve concrete durability – A fundamental view. *In: Fourth International Conference on Sustainable Construction Materials and Technologies (SCMT4)*. Las Vegas, USA, 7–11 August.

Kearsley, E.P., 2006. The use of foamcrete for affordable development in third world countries. In: Dhir, R.K. and McCarthy, M.J. (eds.) *Concrete in the Service of Mankind: Appropriate Concrete Technology*, Vol. 3. Milton Park: Taylor and Francis, pp. 232–242.

Kearsley, E.P. and Wainwright, P.J., 2001. The effect of high fly ash content on the compressive strength of foamed concrete. *Cement and Concrete Research*, 31(1), pp. 105–112. https://doi.org/10.1016/S0008-8846(00)00430-0

Kim, J., Na, S., Zhang, W., Sagawa, T. and Hama, Y., 2017. Effect of limestone powder and gypsum on the compressive strength mixture design of blast furnace slag blended cement mortar. *Journal of Advanced Concrete Technology*, 15(2), pp. 67–80. https://doi.org/10.3151/jact.15.67

Kunhanandan Nambiar, E.K. and Ramamurthy, K., 2008. Fresh state characteristics of foam concrete. *Journal of Materials in Civil Engineering*, 20(2), pp. 111–117. https://doi.org/10.1061/(ASCE)0899-1561(2008)20:2(111).

Lin, R.-S., Liao, Y., Han, Y., Oh, S., Park, K.-B., Yang, H.-M., Wang, X.-Y., Yang, B. and Meng, L.-Y., 2023. Low-CO2 optimization design of quaternary binder containing calcined clay, slag, and limestone. *Materials*, 16(19), 6385. https://doi.org/10.3390/ma16196385

Loon, L.Y., Zaidi, A.M.A., Boon, K.H., Sulaiman, S., Adnan, S.H. and Rahman, I., 2010. Carbonation and water permeability of foamed concrete. *International Journal of Sustainable Construction Engineering and Technology*, 1(1), pp. 33–46. https://journal.uthm.edu.my/index.php/IJSCET/article/view/48

Lothenbach, B., Scrivener, K. and Hooton, R.D., 2011. Supplementary cementitious materials. *Cement and Concrete Research*, 41(12), pp. 1244–1256. https://doi.org/10.1016/j.cemconres.2011.03.015

Mehta, P.K. and Monteiro, P.J.M., 2006. *Concrete: Microstructure, Properties, and Materials*. 3rd edn. New York: McGraw-Hill.

Mohd Fauzi, M.A.M., Muhd Sidek, M.N. and Mohd Ridzuan, A.R., 2020. Effect of limestone powder as an additive and as replacement of self-consolidating lightweight foamed concrete. *International Journal of Sustainable Construction Engineering and Technology*, 11(1), pp. 253–262. https://doi.org/10.30880/ijscet.2020.11.01.024

Mydin, M.A.O., Hamah Sor, N., Althoey, F., Özkılıç, Y.O., Al Bakri Abdullah, M.M., Isleem, H.F., Deifalla, A.F. and Tawfik, T.A., 2023. Performance of lightweight foamed concrete partially replacing cement with industrial and agricultural wastes: Microstructure characteristics, thermal conductivity, and hardened properties. *Ain Shams Engineering Journal*, 14, 102546. https://doi.org/10.1016/j.asej.2023.102546

Nambiar, E.K.K. and Ramamurthy, K., 2006. Models relating mixtures composition to the density and strength of foam concrete using response surface methodology. *Cement and Concrete Composites*, 28(9), pp. 752–760. https://doi.org/10.1016/j.cemconcomp.2006.06.001

Nordin, S.S., Noor, E.E.M. and Chockalingam, P., 2024. Chemical and thermal analysis of fly ash-reinforced aluminum matrix composites (AMCs). *Journal of Composites Science*, 8(5), p.170. https://doi.org/10.3390/jcs8050170

Pandey, B., Maywad, D., Uikey, P., Rathore, S., Dhurve, V., Chouhan, N. and Dedhia, G., 2023. Use of foam concrete in construction. *International Journal of Innovative Research in Multidisciplinary Physical Sciences*, 11(2), pp. 1–6.

Qu, Z., Liu, Z., Si, R. and Zhang, Y., 2022. Effect of various fly ash and ground granulated blast furnace slag content on concrete properties: experiments and modelling. *Materials*, 15(9), 3016. https://doi.org/10.3390/ma15093016

Ramamurthy, K., Kunhanandan Nambiar, E.K. and Indu Siva Ranjani, G., 2009. A classification of studies on properties of foam concrete. *Cement and Concrete Composites*, 31(6), pp. 388–396. https://doi.org/10.1016/j.cemconcomp.2009.04.006

Remadnia, A., Dheilly, R., Laidoudi, B. and Quéneudec, M., 2009. Use of animal proteins as foaming agent in cementitious concrete composites manufactured with recycled PET aggregates. *Construction and Building Materials*, 23(10), pp. 3118–3123. https://doi.org/10.1016/j.conbuildmat.2009.06.027

Salman, B.A. and Al-Mulali, M.Z., 2025. The effect of nano technology on the properties of sustainable foam concrete. *Journal of Engineering*, 31(6), pp. 193–203. https://doi.org/10.31026/j.eng.2025.06.10

Samad, S. and Shah, A., 2017. Role of binary cement including supplementary cementitious material (SCM), in production of environmentally sustainable concrete: A critical review. *International Journal of Sustainable Built Environment*, 6(2), pp. 663–674. https://doi.org/10.1016/j.ijsbe.2017.07.003

She, W., Du, Y., Zhao, G., Feng, P., Zhang, Y. and Cao, X., 2018. Influence of coarse fly ash on the performance of foam concrete and its application in high-speed railway roadbeds. *Construction and Building Materials*, 170, pp. 153–166. https://doi.org/10.1016/j.conbuildmat.2018.02.207

Schöler, A., Lothenbach, B., Winnefeld, F. and Zajac, M., 2015. Hydration of quaternary Portland cement blends containing blast-furnace slag, siliceous fly ash and limestone powder. *Cement and Concrete Composites*, 55, pp. 374–382. https://doi.org/10.1016/j.cemconcomp.2014.10.001

Sebastian, M.S. and V R, T.R., 2021. An investigation on geopolymer concrete with GGBFS and fly ash. *International Journal of Engineering Research & Technology*, 9(12), pp. 213–216. http://www.ijert.org.

Vashistha, P., Park, S. and Pyo, S., 2022. A review on sustainable fabrication of futuristic cementitious binders based on application of waste concrete powder, steel slags, and coal bottom ash. *International Journal of Concrete Structures and Materials*, 16(1), 32. https://doi.org/10.1186/s40069-022-00541-9

Vishavkarma, A., Kumar, M. and Harish, K.V., 2024. Influence of combined substitution of slag and fly ash in improving the pore structure and corrosion resistance of foam concrete mixtures used for reinforced concrete applications. *Case Studies in Construction Materials*, 21, e03449. https://doi.org/10.1016/j.cscm.2024.e03449

Wee, T.H., Babu, D.S., Tamilselvan, T. and Lim, H.S., 2006. Air-void system of foamed concrete and its effect on mechanical properties. *ACI Materials Journal*, 103(1), pp. 45–52.

Yohans, J., Rangan, P.R., Ambun, E. and Tumpu, M., 2024. Mechanical properties of foamed concrete (FC) using high-volume fly ash. *International Journal of GEOMATE*, 26(118), pp. 141–148. https://doi.org/10.21660/2024.118.g13323

Zhang, S., Qi, X., Guo, S., Zhang, L. and Ren, J., 2022. A systematic research on foamed concrete: the effects of foam content, fly ash, slag, silica fume and water-to-binder ratio. *Construction and Building Materials*, 339, 127683. https://doi.org/10.1016/j.conbuildmat.2022.127683

Zhang, D., Hao, W. and Yang, Q., 2023. Experimental study on the application of recycled concrete waste powder in alkali-activated foamed concrete. *Materials*, 16(17), 5728. https://doi.org/10.3390/ma16175728

Zhang, Z., Li, L., Nong, Q., Li, J. and Li, B., 2026. A new insight into moisture transport in foamed concrete: Coupled effects of density and fly ash. *Construction and Building Materials*, 506, 144925. https://doi.org/10.1016/j.conbuildmat.2025.144925

Zhang, Z., Provis, J.L., Reid, A. and Wang, H., 2015. Mechanical, thermal insulation, thermal resistance and acoustic absorption properties of geopolymer foam concrete. *Cement and Concrete Composites*, 62, pp. 97–105. https://doi.org/10.1016/j.cemconcomp.2015.03.013

Zhou, G. and Su, R.K.L., 2023. A review on durability of foam concrete. *Buildings*, 13(7), 1880. https://doi.org/10.3390/buildings13071880

## Appendix A

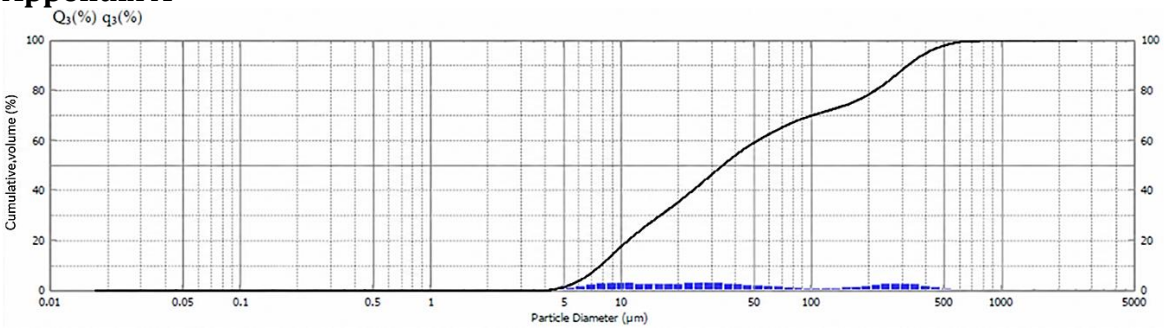



**Figure A1.** Particle size distribution of fly ash, showing the median particle size (D50).

# مزيج رباعي جديد لخرسانة رغوية صديقة للبيئة

**سارة عبد الرضا حسن *، محمد زهير الملالي**

قسم الهندسة المدنية، كلية الهندسة، جامعة بغداد، بغداد،العراق

**الخلاصة**

تتقصى هذه الدراسة سبل تطوير خرسانة رغوية مستدامة وعالية الأداء من خلال استخدام نظام رباعي كبديل جزئي للإسمنت. يقيّم البحث استبدال الإسمنت بالرماد المتطاير كمادة إحلال رئيسيه، مع دمج خبث الأفران ومسحوق الحجر الجيري (كمكونات ثانوية)، وذلك بنسب استبدال بلغت 20%، 30%، و40.%. تم تحضير أربعة خلطات ومن ضمنها الخلطة المرجعية من الخرسانه الرغويه بكثافه طازجه مستهدفه تصل إلى 50±1350كجم/م³ وبنسة بخلط (1:1.2:0.45) وتم اجرا تقييم شامل للخرسانة الرغوية من حيث الكثافه الطازجه، ومقاومة الانضغاط، ومقاومة الشد بالانفلاق، وعمق الكربنة، إلى جانب التوصيف المجهري باستخدام المجهر الإلكتروني الماسح .(SEM) أظهر تحليل SEM أن الخلطة ذات نسبة الاستبدال البالغة 40% طورت بنية مجهرية كثيفة ومترابطة، تميزت بتكوّن هلامات ثانوية من C–S–H و C–A–S–Hوكشفت النتائج التجريبية أن نسبة الاستبدال البالغة 40%حققت الأداء الأكثر تميزاً، حيث وصلت مقاومة الضغط إلى 9 ميجا باسكال عند عمر 28 يوماً، متجاوزة بذلك أداء الخلطة المرجعية بشكل فعال .علاوة على ذلك، حقق هذا المزيج الرباعي المحدد مقاومة شد بالانفطار بلغت 1.35 ميجا باسكال ولكنها بم تتفوق على المرجعية بمقاومة شد الانفطار,ومعذلك حققت كثافه طازجه محسنة قدرها 1345 كجم/م³، مما ضمن استقراراً فائقاً للرغوة. وتؤكد هذه النتائج أن استبدال الإسمنت بنسبة 40% بهذا الرابط الرباعي يوفر حلاً صديقاً للبيئة لإنتاج خرسانة رغوية مستقره وعاليه المقاومة، مما يجعلها ملائمة للتطبيقات شبه الإنشائية

**الكلمات المفتاحية:** الخرسانه الرغويه ، الاستبدال الرباعي ، الرماد المتطاير، الاستدامه ، مقاومه الانضغاط